Online characterization of moisture transport in a high-performance carbon fiber-reinforced thermoplastic composite at high temperatures: Identification of diffusion kinetics

Luc Amedewovo, Arthur Levy, Basile de Parscau Du Plessix, Laurent Orgeas, Steven Le Corre

Online characterization of moisture transport in a high-performance carbon fiber-reinforced thermoplastic composite at high temperatures: identification of diffusion kinetics

Luc Amedewovo[a], Arthur Levy[a,*], Basile de Parscau du Plessix[a], Laurent Orgeas[b], Steven Le Corre[a]

[a] *Nantes Université, IRT Jules Verne, CNRS, Laboratoire de thermique et énergie de Nantes, LTeN, UMR 6607, F-44000 Nantes, France.*
[b] *Univ. Grenoble Alpes, CNRS, Grenoble INP, 3SR Lab, 38000 Grenoble, France*

Abstract

Prior to processing, high-performance fiber-reinforced ThermoPlastic matrix Composites (TPC) are usually stored in ambient conditions, thus causing moisture sorption. During processing at high temperature, the stored moisture induces defects that deteriorate the mechanical properties of the produced parts. In order to understand these effects, it is necessary to study water (de)sorption phenomena in TPC, which was only characterized at low temperatures up to now ($< 100°C$). Thus, we characterized online moisture (de)sorption mechanisms at high temperatures (up to 300°C) on large and representative samples of a high-performance carbon-fiber (CF) reinforced PolyEtherKetoneKetone (PEKK) laminates. This characterization was performed thanks to a new thermogravimetric device named OMICHA (Online Moisture Ingress CHAracterization) that we developed purposely. This new device allows to continuously measure weight variation of large composite samples under controlled and high temperature and/or humid environment. Sorption and desorption tests allowed to determine macroscopic moisture diffusion coefficient of CF/PEKK at several temperatures, highlighting a complex dual stage macroscopic diffusive behavior which is also modeled and discussed.

Keywords: A. Laminate, A. CF/PEKK, B. Hygro-thermal effect, B. Environmental Degradation, D. Thermogravimetric analysis (TGA)

1. Introduction

Due to their high specific mechanical properties, advanced fiber-reinforced polymer composites are increasingly used in aircraft and aerospace industries. Although thermoset polymers are currently the most widely used in composites, novel high-performance thermoplastic polymers are being introduced to manufacture fiber-reinforced ThermoPlastic matrix Composites (TPCs). TPCs exhibit several advantages over thermoset matrix composites, *e.g.*, in terms of weldability and shelf (storage) life. In addition, high-performance

*Corresponding author
Email address: arthur.levy@univ-nantes.fr (Arthur Levy)

polymers exhibit good mechanical properties which meet the aeronautical specifications. They also have high glass transition temperature (T_g) and high melting temperature (T_m) that allow high service temperatures (in general up to 250°C). Finally, they have a good chemical resistance to solvents. Classical high-performance thermoplastic polymers used in TPCs are PolyEtherEtherKetone (PEEK) and PolyEtherKetoneKetone (PEKK). They are semi-crystalline polymers with an aromatic structure which confers them the aforementioned properties. However, the processing of high-performance TPCs requires high temperatures (between 330°C and 400°C) unlike thermoset composite (between 120°C and 175°C). This makes their manufacturing challenging.

Several studies carried out on thermoset matrix composites have revealed that thermoset polymers uptake water when subjected to a humid environment [1, 2, 3, 4]. The moisture sorption usually occurs during the storage of the composites before processing. During processing at high temperature, the initial moisture stored inside the composites provides pores nucleation sites which can lead to the formation of defects (delaminations, voids, *etc.*) [5, 6, 7]. Although high-performance TPCs generally uptake less water than high-performance thermoset matrix composites [8, 9, 10], the effect of moisture is not negligible. To avoid this detrimental effect of moisture, understanding of the moisture (de)sorption mechanisms, especially the moisture diffusion kinetics in the material is required. Moisture (de)sorption in fiber-reinforced thermoset polymer composites has been widely studied in the literature [11, 12, 13, 14, 15, 16, 17]. On the contrary, there are very few studies dedicated to (de)sorption mechanisms in TPCs [18, 19, 20, 21, 22, 23]. Most of them focused on CF/PEEK. Only five recent articles have been found on CF/PEKK [24, 25, 26, 27, 28]. In most of these studies (de)sorption is characterized at low and constant temperatures, either in a humid atmosphere or in water. Since high-performance TPCs are processed at high temperatures, a characterization of moisture desorption at high temperatures is required.

The traditional method used to characterize moisture (de)sorption is to measure the weight variation of a specimen exposed to a controlled temperature and humidity environment, through gravimetric measurements. These measurements are made at periodic time intervals, by using a weighing scale (static gravimetric method) [14, 29]. This technique is labor intensive since the samples must be taken out of the testing environment at various times and over a long period of time, for external weighing. Moreover, the handling time outside the test environment can be a significant source of error. To overcome these limitations, another technique used in the literature is the Dynamic Vapor Sorption (DVS) method [30, 31]. DVS instruments operate by flowing precisely controlled concentrations of water vapors in dry air over a sample at a known flow rate and temperature. The sample is supported, through a sample holder, by a digital micro weighing scale which detects the sorption or desorption of water vapor through the increase or decrease of the material weight, as the relative humidity varies (dynamic gravimetric method). The benefit of this technique is to provide a continuous and automatic, *i.e.*, online, measurement of the weight variation which makes it widely used in fields such as the pharmaceutical, food, textile production or building materials (concrete)

[32, 33]. However, this technique is limited to small sample sizes (up to 8 mm × 8 mm) and low sample weights (up to 5 g) [34]. This is detrimental for TPCs which require larger sample size to get representative characterization of moisture (de)sorption mechanisms. Moreover, the maximum temperature that can be reached on these devices are 200°C which is also a drawback for TPCs. Standard ThermoGravimetric Analysis (TGA) equipment allows to largely exceed this temperature but here again, the required sample size is also too small (about 4 mm in diameter) to allow proper and representative characterization of moisture (de)sorption in TPCs.

For these reasons, we developed a new thermogravimetric device to perform moisture sorption and desorption tests at temperatures above 200°C on large and representative samples of TPCs. This new device was used to characterize the moisture desorption mechanisms at high temperatures on an aerospace grade CF/PEKK7002 composite laminate.

2. Materials

CF/PEKK prepreg plies supplied by Toray Advanced Composite were used to produce consolidated laminates. The plies have a fiber areal weight (FAW) of 194 g·m^{-2} and a theoretical thickness of 0.185 mm. The PEKK mass content is 34 %. The glass transition temperature (Tg), melting temperature (Tm) and crystallization temperature (Tc) of PEKK 7002 are respectively 160°C, 337°C, and 265°C (according to the manufacturer). In practice, the melting zone, observed during Differential Scanning Calorimetry (DSC) experiments, extends between 310°C and 360°C, with a melting peak at 338°C. In non-isothermal conditions, the crystallization zone extends between 240°C and 283°C, with a crystallization peak at 269°C. This melting and crystallization range can also be found in [35, 36, 37].

From the prepreg plies, $[0]_{16}$ laminates were consolidated in a hot press. The 348 mm × 348 mm prepreg plies were stacked in a picture-frame mold (internal cavity dimensions: 350 mm × 350 mm) and consolidated on a 50 t Pinette P.E.I press according to the following cycle: heating at 10°C/min up to 380°C under a pressure of 0.1 MPa; the temperature was held for 20 min under a pressure of 4 MPa; cooling at 10°C/min at the same pressure, then demolding. The final part dimensions after consolidation are 350 mm × 350 mm × 2.90 mm. This final size of the laminate is due to the high pressure and the clearance between the plies and the internal cavity of the mold which promotes PEKK resin squeeze out.

Since a significant porosity content has a significant influence on the moisture diffusion kinetics [38, 39, 40], optical micrographs of the consolidated laminates validate the negligible porosity content after the consolidation (Figure 1). To perform microscopic observations, the samples were encapsulated using a slow-curing epoxy resin (EpoFix, Struers). The samples were then prepared using traditional grinding and polishing techniques on an automated polishing machine (Tegrapol-21 and TegraForce-5, Struers) and observed on the digital microscope KEYENCE VHX-7000 series. The cross section micrographs were ob-

Figure 1: Micrograph (cross section parallel to the fibers main axis) of the consolidated samples before deconsolidation tests. The initial porosity content is not measurable.

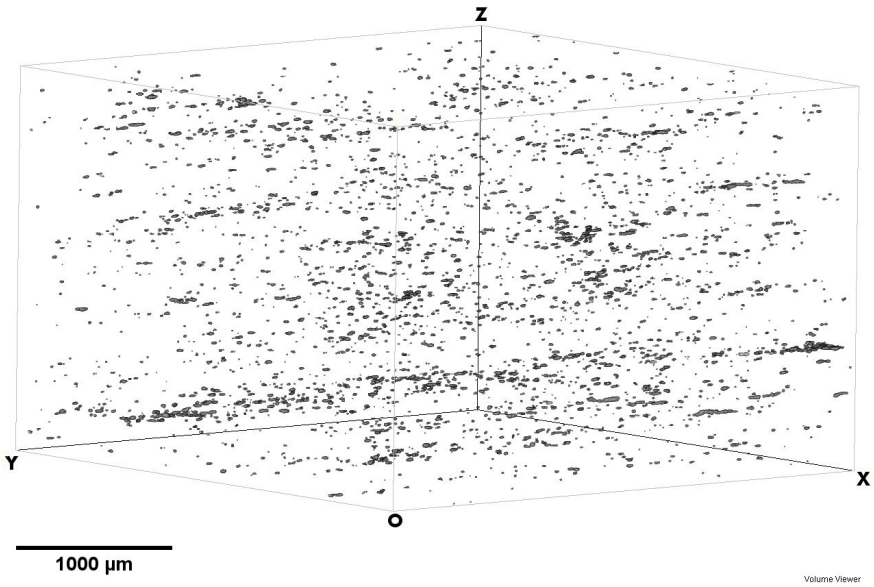

Figure 2: 3D image of the porosity distribution in a sample of 20 mm diameter cut from the consolidated laminate (Region Of Interest size: 1000×1000×650 pixels). The porosity content is 0.02 %.

tained by assembling several sections with a resolution of 2880 px × 2160 px (objective magnification ×200) resulting in an image with a large area of observation and a good resolution. Using the trainable weka segmentation algorithm [41] in an image processing software (Fiji), the porosity content was measured.

This microscopic observation was validated by a micro-CT analysis which showed an initial porosity content of 0.02 % (Figure 2). This value is a minor of the laminate porosity content. The 3D image of the sample (20 mm diameter) was obtained on one of the X-ray tomographs of the ID19 line at European Synchrotron Radiation Facilities (Grenoble, France). The raw 3D image was produced (i) with a voxel size of 3.81^3 μm^3 and a large observation zone (2016×2016×1410 pixels), (ii) by using Paganin method [42]. Additional post-treatment on a Region Of Interest (ROI) of 1000×1000×650 pixels (picked from the raw 3D image) using the trainable weka segmentation algorithm, in an image processing software (Fiji), allowed to measure the porosity content.

3. Online Moisture Ingress CHAracterization bench (OMICHA)

Sorption or desorption tests consist in measuring the weight gain or loss of a sample under controlled temperature and hygrometry conditions. In the case of desorption tests, the initially wet sample is dried at a given isotherm and constant relative humidity until the sample is completely dried. In the case of sorption tests, the initially dry sample is moisturized in an environment with a known constant relative humidity and temperature.

Usually, sorption tests are carried out in climatic chambers. The Relative Humidity (RH) is set either by using relative humidity generators or by saturated water solutions of properly selected salts. These salts are selected in the Greenspan table which gives the equilibrium relative humidity of Saturated Salt Solutions from 0 to 100°C [43]. During the sorption tests, the weight changes are measured at different times on an external weighing scale in accordance with the standard ASTM D5229/D5229M (static gravimetric method). This makes this method laborious and the existing online weighing methods (DVS and standard TGA) require small samples that are not representative of composite structures. In order to overcome the limitations of these methods, a new device for the characterization of moisture diffusion kinetics has been developed.

3.1. Bench development

OMICHA (Online Moisture Ingress CHAracterization) device has been developed to measure continuously the weight of samples of a size representative of a structure scale (up to 150 mm × 150 mm), in a controlled hygrothermal environment.

3.1.1. Design

As shown in Figure 3, the device is composed of an oven (Heratherm OGH60 from Thermo Scientific), a sample holder made of aluminum and a semi-micro weighing scale (Explorer EX125M from OHAUS) with an accuracy of 0.01 mg, in accordance with the ASTM D5229/D5229M standard. The whole device was placed on a marble table to avoid the influence of external vibrations on the weight measurements. The oven allows to heat up to 330°C by natural convection. A suspended sample holder was specifically designed and manufactured, in order to transfer the samples weight to the semi-micro weighing scale. A metallic tip was connected to the upper extremity of the sample holder, in order to avoid force torque at the contact zone between the weighing scale and the sample holder. The stability of the sample holder was provided by a counterweight placed at its lower extremity. Due to the total weight of the sample holder and the counterweight (83.26 g), the measuring range of the weighing scale was reduced from 120 g to 36.74 g.

3.1.2. Heat management

To prevent high heat exchanges along the aluminum sample holder which may result in condensation and artifacts, the sample holder was made of two parts connected by a polycarbonate insulator shaft. Since

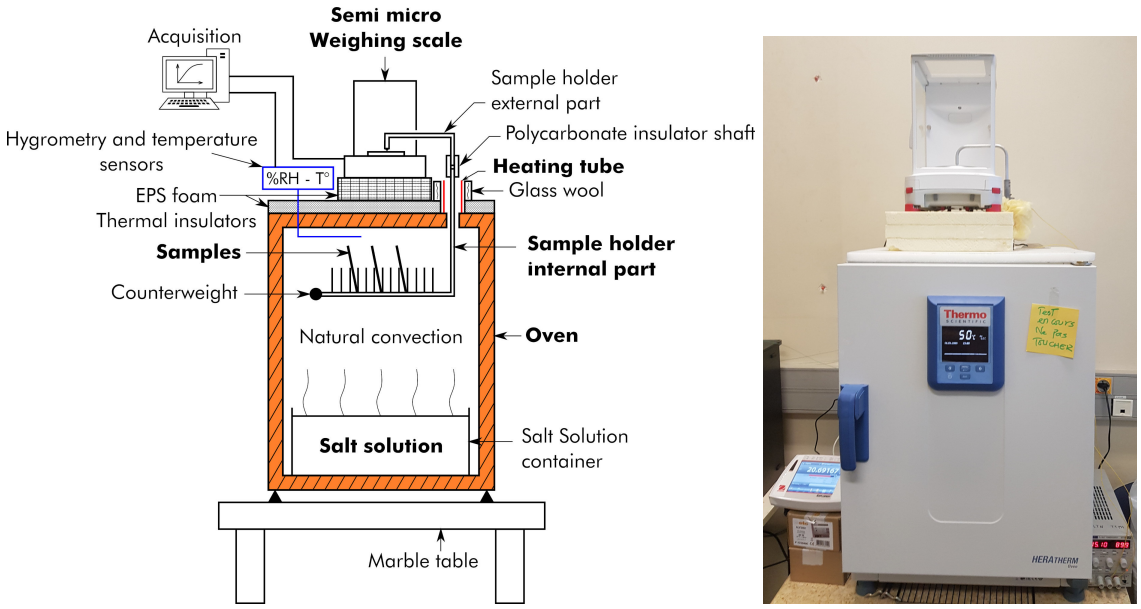

Figure 3: Online moisture ingress characterization (OMICHA) bench. (left) Schematic view and (right) setup picture.

polycarbonate has a low thermal conductivity ($\approx$ 0.04 W·m^{-1}·K^{-1} [44]), the shaft allowed to insulate thermally the external part of the sample holder from its internal part which is in the oven. The weighing scale was also thermally insulated from the oven by means of Expanded PolyStyrene (EPS) foam.

With respect to external environment of the setup, there was no significant variation of ambient temperature (23°C measured with a K-type thermocouple) and atmospheric pressure (0.1 MPa or 1.024 bar measured by a pressure sensor, from Keller's 35XTC series) during the experiments.

3.1.3. Humidity management

During sorption tests, the moisture in the oven was provided by a saturated salt solution selected from the Greenspan table. The saturated salt container was let in the oven during the whole experiment. The container volume is large enough (14×10^{-3} m^3) to avoid refilling with salt solution during a test. A heating tube surrounded by glass wool was placed at the exit of the sample holder out of the oven. This heating tube was used to heat locally the water vapor which escaped from the oven and thus prevented water condensation on the sample holder.

The OMICHA bench was used in two different configurations, *i.e.*, sorption at low temperature and desorption at high ones. The saturated salt container is not used in desorption configuration, since the environment in the oven had to be dried. We did not performed sorption tests above 100°C, as these tests would require an additional pressure: this was not possible here.

3.1.4. Measurements

The temperature and the relative humidity were respectively measured by K-type thermocouple and a thermohygrometer (TH 210-R from Kimo) with an accuracy of ± 1.5 %RH. The weight, temperature and relative humidity measurements were synchronized and performed automatically using a single piece of software developed on labVIEW. The weight variation Δw (%) over time was calculated from the weight measurements according to the following equation (1):

$$\Delta w(t) = \left(\frac{w(t) - w(0)}{w(0)} \right) \times 100 \quad (1)$$

where $w(t)$ and $w(0)$ are the actual and initial sample weights, respectively.

Compared to the small sample sizes (up to 8 mm × 8 mm) and low sample weight (up to 5 g) required in DVS and TGA methods, the OMICHA device sample holder can support large size samples up to 150 mm × 150 mm × 10 mm with a weight up to 36 g. Additionally, desorption tests on OMICHA can be performed up to 330°C (which is in the melting zone of the studied material).

3.2. Validation

The weighing scale used on the OMICHA device was pre-calibrated by the supplier and has an accuracy of 0.01 mg. To evaluate the effect of the sample holder on the measurement, several objects were weighed directly on the pan of the weighing scale without the sample holder. The weight values obtained from these measurements were used as reference. The same objects were weighed by mean of the sample holder, in ambient conditions. Since there are fifteen positions available on the sample holder, the samples were placed at the middle of the sample holder. Figure 4 left shows the relative error between the measurements with the sample holder and the reference weights. All the weighing were performed three times. The error bars plotted in Figure 4 represent the standard deviation. The relative error related to the use of the sample holder decreases with increasing sample weight. First, for low weight samples (inferior to 0.01 g), the relative error is superior to 5 %. Second, for samples weight between 0.01 g and 1 g, the maximum relative error is 4 %. Finally, over 1 g, the maximum relative error is 0.03 %. As discussed hereunder, such a precision enables to properly characterize moisture diffusion kinetics with the targeted composite sample size (80 mm × 80 mm) and weights (≈ 30 g).

In addition, a heating test at 180°C was performed without any sample on the sample holder. During this test, the oven was heated to 180°C and maintained at this temperature. As shown in Figure 4 right, during the ramp-up, some weight variations can be seen with a low magnitude (0.007 %). These variations are attributed to convective effect in the oven. As soon as the temperature reaches the dwell temperature, a weight loss is observed. This weight loss stabilizes after a time period and remains constant during the whole dwell. This observation under isothermal condition is probably attributed to a desorption of the aluminum sample holder. However, the weight variation stabilization shows that at isothermal temperature,

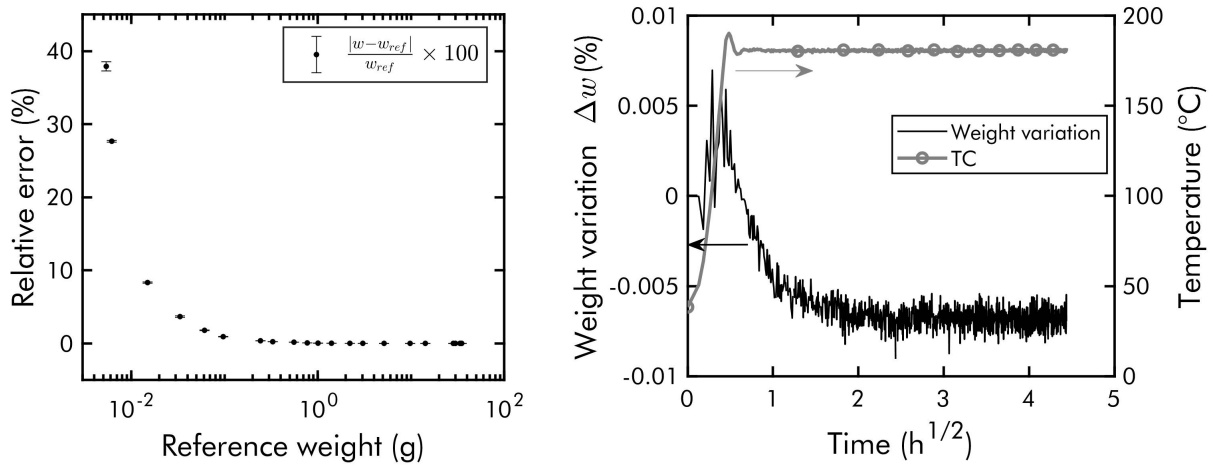

Figure 4: OMICHA measurements validation. (left) Relative error (%) for different reference weights and (right) effect of the oven temperature on the weight variation Δw.

the temperature inside the oven has almost no influence on the measurement of the weighing scale. It also highlighted the efficiency of the insulation system. For these reasons, before all measurement on the OMICHA device, the system is preheated up to the target temperature until weight variation stability is reached, before the sample positioning. This is illustrated in Figure A.9 (see Appendix A), which shows a negligible weight variation Δw evolution ($\pm$0.004 %) of the sample holder exposed to a low temperature of 40°C and 65 %RH for 2 hours before the samples positioning.

4. CF/PEKK laminate characterization procedure

Using the OMICHA device, desorption tests were carried out on 80 mm $\times$ 80 mm $\times$ 2.90 mm composite samples cut from the press consolidated laminates. All the samples were cut from the laminates after consolidation, by water jet cutting on a ProtoMAX abrasive waterjet machine. The samples were then cleaned with a cloth and stored in ambient conditions ($\approx$ 23°C and 50 %RH) for 5 months. Before each desorption test, the oven was preheated to the defined temperature for the test. As mentioned earlier, the saturated salt container is removed from the oven in the desorption configuration. The defined temperatures for the desorption tests are listed in table 1.

After the oven preheating, the desorption test was performed on a single sample placed in the middle of the sample holder. The time evolution sample weight was recorded and the corresponding weight variation Δw was determined according to equation (1). The initial weights ranged from 29 g to 30 g. All the desorption tests were performed under air atmosphere, in order to be representative of the atmosphere in which the composite is processed.

Desorption tests have been carried out to analyze the moisture desorption kinetics at high temperatures.

Table 1: Desorption and sorption tests parameters. T_g corresponds to the material glass transition temperature and T_c its lowest crystallization temperature.

Desorption		Sorption	
Range	Temperature	Relative humidity	Temperature
$T < T_g$	140°C		
$T_g < T < T_c$	180°C, 200°C	65 %	40°C
$T \geq T_c$	250°C, 300°C		
Sample: consolidated laminate		Sample: 7 × 1 tape	

In order to characterize the moisture sorption kinetics at a lower temperature, sorption tests were performed at 40°C and 65 %RH. To limit the duration of the test, sorption tests were not performed on laminates but rather directly on a prepreg ply (80 mm × 80 mm × 0.2 mm).

Before sorption tests, a salt solution was prepared by mixing a Sodium Chloride salt (NaCl) with a hot distilled water at 80°C. A fully saturated solution was obtained when the NaCl salt can no longer dissolve in the water. The resulting salt solution was then cooled down to the testing temperature (40°C) by natural convection and placed in the preheated oven. When the humidity reached equilibrium in the oven, samples were positioned on the sample holder. The relative humidity at equilibrium (65 %RH) was given by the thermohygrometer placed in the oven. Since the weight of a single prepreg ply was less than the weight of a laminate, the sorption test was performed on a set of seven samples of one tape (80 mm × 80 mm × 0.2 mm) in order to obtained a mean weight variation value. The time evolution of the samples weight was recorded and the corresponding weight variation was also determined according to equation (1). This sorption procedure was repeated twice.

5. Results

5.1. Desorption tests

Figure 5 shows the evolution of the weight variation Δw of tested samples with the square root of time $\sqrt{t}$ obtained at different temperatures. Since the laminates used in this study were initially consolidated at 380°C, it is assumed that there were no residual volatiles from additives such as plasticizers present in the tested samples. In fact, most additives evaporated during the initial laminate consolidation process. The observed weight losses are thus attributed to the desorption of the moisture initially stored in the polymer matrix, during the laminate consolidation and during the storage in an ambient condition.

This figure shows that during all tests performed at temperature T≤200°C, the weight loss stabilizes after a certain time and exhibit a Fickian-like time evolution. Instead, at T>200°C, a dual stage time

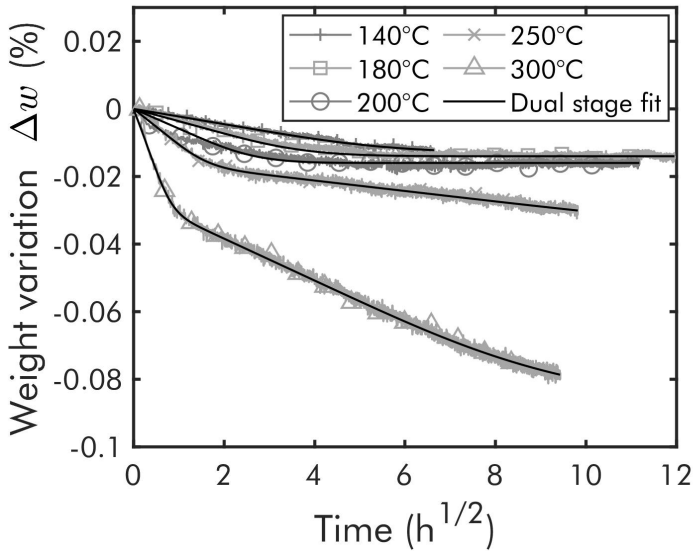

Figure 5: Desorption curves. Evolution of the weight variation Δw of tested samples with the square root of time $\sqrt{t}$ at different constant heating temperatures.

evolution [45] is observed: a first rapid weight decrease (similar to the one observed at T$\leq$200°C) is followed by a slower one which does not reach a stabilization for the duration of our tests.

5.2. Thermal degradation

In order to verify whether the weight variation above 200°C can reach a stabilization, a first desorption test was performed at 250°C on a sample already dried at 180°C for 72h. The objective was to verify if drying at 250°C could tend towards stabilization for longer exposure times. Figure 6 (left) shows that even after 16 days of exposition at 250°C, no stabilization was reached. A second desorption test was performed at a higher temperature of 325°C on a sample already dried at 300°C for 24h. The objective of this test was to check if the stabilization could be reached faster at higher temperature. The initial drying was done in order to reach the second stage of desorption. Figure 6 (right) shows that even at a temperature in the material melting zone (325°C), the weight variation does not reach a stabilization. Conversely, the weight loss is accelerated when melting is reached. This observation supports the fact that dual stage diffusion, in polymer composites, hardly reaches equilibrium [45]. In fact, a longer exposition of this type of material to such high temperatures (T$\geq$ 250°C) lead to the material degradation [23, 46].

Several authors have studied the degradation phenomenon and showed that it is due to the scission of macromolecular chains of the polymer matrix which generate volatiles and radicals [47, 48]. The desorption of the volatiles produced by the chains scission explains the second slope observed on the desorption curve at 325°C (Figure 6 right). The authors also showed that when the material is maintained at such high

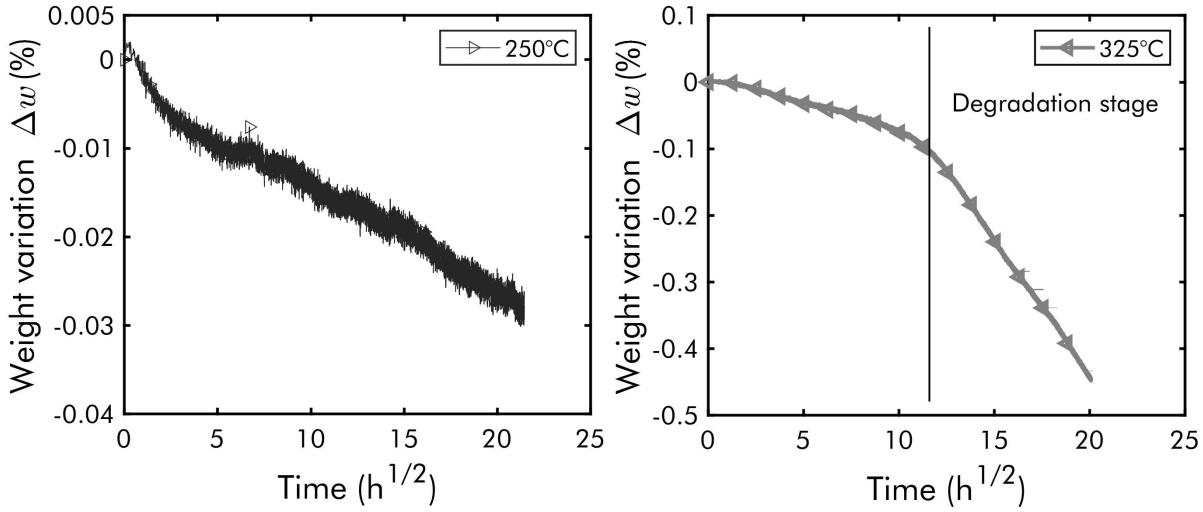

Figure 6: Evolution of the weight variation Δw of tested samples with the square root of time $\sqrt{t}$ for a test performed at 250°C with a sample initially dried for 72h@180°C (left) and at 325°C with a sample initially dried for 24h@300°C (right). The polymer matrix degradation occurs after long exposition at 325°C.

temperatures (T$\geq$ 250°C) for a long time, the radicals resulting from the chains scission can recombine together to form crosslinks. The polymer macromolecules then start branching.

5.3. Sorption tests

The obtained sorption curves shows weight increase vs time (Figure 7). First, a good repeatability of the sorption tests is observed. The maximum absolute difference between the weight variation obtained for both tests is only 0.01 %. Second, the duration of the test is not long enough to confirm a total saturation of the samples. In addition, the reported curves can be divided into two stages. As for the desorption curves, the first stage is relatively fast (couple of hours) and is represented by the initial slope. Similar behavior has also been observed, in the literature, on CF/PEEK composite [20, 18] and on CF/PEKK composite, placed under more severe conditions (80°C at 90 %RH [26], and water immersion at 70°C [25]).

Additionally during the second stage of the sorption test, a sudden increase of the weight was observed around $t = 6^2$ h. This localized behavior is different from the monotonic behavior observed in the desorption tests. This behavior was also observed in the literature by Suh *et al.* [49] on a cured CF/epoxy composite immersed in water at 70°C. This Non-Fickian behavior suggests the presence of another physical phenomenon in sorption, but further analysis of this is not considered within the scope of this work. Only the first stage of the sorption curve was thus considered to determine the diffusion kinetics at early stages.

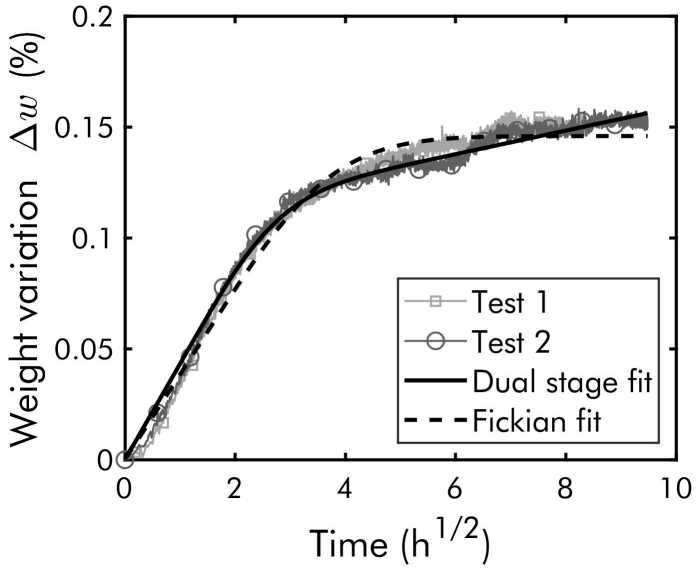

Figure 7: Sorption curves. Evolution of the weight variation Δw of tested samples with the square root of time $\sqrt{t}$ during two moisture sorption tests performed at 40°C and 65 %RH on seven samples of one prepreg ply.

6. Moisture transport mechanisms and macroscopic modeling

The CF/PEKK material studied is an industrial complex system involving several heterogeneities such as microporosities and fiber interfaces with undetermined sizing. Thus moisture transport mechanisms in these complex heterogeneous systems may involve adsorption, absorption, swelling or relaxation, capillary effects at small scales together with diffusion phenomena at smaller molecular scales. Nonetheless, the time evolutions of weight variations we reported in Figures 5 and 7 lead us to approach these complex possible micro-scale mechanisms by diffusive processes at the macro-scale. Thus, given the plate geometry of the tested samples, and by reasonably assuming that moisture transport only occurs along the thickness direction x of the samples, a possible diffusive transport model is the well-known Fick model, which is written for a one-dimensional (1D) case as:

$$\frac{\partial C}{\partial t} = D\frac{\partial^2 C}{\partial^2 x} \tag{2}$$

where C is the water concentration, D ($\mathrm{m^2{\cdot}s^{-1}}$) the diffusion coefficient. D is assumed to be independent of the concentration C. The resolution of equation (2) in a plane sheet with an initial uniform water concentration C_0 and which is subjected to a constant water concentration C_1 at its upper and lower faces is given by Crank [50]:

$$\frac{C - C_0}{C_1 - C_0} = 1 - \frac{4}{\pi}\sum_{n=0}^{\infty}\frac{(-1)^n}{(2n+1)}\exp\left(-\frac{D(2n+1)^2\pi^2 t}{l^2}\right)\cos\left(\frac{(2n+1)\,\pi x}{l}\right) \tag{3}$$

where l the sample thickness. This solution was obtained by assuming C_0 to be initially uniform in the sample and C_1 constant because the water concentration in the sample environment is at saturation.

If M denotes the actual total amount of water absorbed or desorbed by the sample, and M_∞ the same quantity after infinite time (at saturation or equilibrium), then by integrating equation (3) over the thickness l, the following equation is obtained:

$$M = M_\infty \times \left\{ 1 - \frac{8}{\pi^2} \sum_{n=0}^{\infty} \frac{1}{(2n+1)^2} \exp\left(-\frac{D(2n+1)^2 \pi^2 t}{l^2} \right) \right\} \tag{4}$$

or

$$M = M_\infty \times \left\{ 2 \left(\frac{Dt}{l^2} \right)^{\frac{1}{2}} \left(\pi^{-\frac{1}{2}} + 2 \sum_{n=1}^{\infty} (-1)^n \mathrm{ierfc} \frac{nl}{(Dt)^{\frac{1}{2}}} \right) \right\} \tag{5}$$

with

$$\frac{M}{M_\infty} = \frac{w - w_0}{w_\infty - w_0} \tag{6}$$

where w_0 and w_∞ are respectively the initial sample weight and the sample weight at equilibrium.

For short times, *i.e.*, when $t \ll \frac{\pi l^2}{16D}$, equation (5) can be simplified:

$$M = M_\infty \times \left\{ \frac{4}{\pi^{\frac{1}{2}}} \left(\frac{Dt}{l^2} \right)^{\frac{1}{2}} \right\} \tag{7}$$

Consequently, by plotting the weight variation as function of square root of time as in figure 5 and 7, the diffusion coefficient can be determined from the tangent S_l at the origin of the curve recorded during (de)sorption experiments:

$$D = \pi \left(\frac{l}{4M_\infty} \right)^2 (S_l)^2 \tag{8}$$

The Fick model can be used to represent the diffusion mechanisms in the composite sample below 200°C during desorption. As shown by the desorption curves above 200°C (Figure 5), the weight variation does not reach a stabilization after the first linear stage. In order to take into account this behavior change at high temperatures, the Langmuir-type [51] model can be used. However, the identification of this model parameters is complex. In this study, a phenomenological model called "dual stage" was adopted. This model, described by the equation (9), is based on the assumption that two decoupled Fickian diffusion operate simultaneously with two diffusion coefficients, D_1 and D_2 respectively associated with two different water concentrations C_1 and C_2 [52]. The first one is introduced to moisture diffusion in the early stage and the second one for diffusive process in an second stage. This model is deduced from equation 2, by considering $C = C_1 + C_2$ (superposition of two Fickian diffusion). It is the most used to describe the diffusion mechanisms in epoxy matrix composites [15, 52, 53].

$$\frac{\partial C_1}{\partial t} + \frac{\partial C_2}{\partial t} = D_1 \frac{\partial^2 C_1}{\partial^2 x} + D_2 \frac{\partial^2 C_2}{\partial^2 x} \tag{9}$$

Table 2: Dual stage model parameters

Temperature (°C)	D_1 ($m^2 \cdot s^{-1}$)	$M_{\infty,1}$ (%)	D_2 ($m^2 \cdot s^{-1}$)	$M_{\infty,2}$ (%)	Comments
40	0.24×10^{-12}	0.106	-	-	Sorption test
140	14.46×10^{-12}	-0.013	0	0	Desorption test
180	32.47×10^{-12}	-0.014	0	0	Desorption test
200	63.87×10^{-12}	-0.016	0	0	Desorption test
250	174.68×10^{-12}	-0.015	1.99×10^{-12}	-0.024	Desorption test
300	660.49×10^{-12}	-0.026	4.93×10^{-12}	-0.061	Desorption test

The solution of equation (9) is deduced from the analytical solution (Equation 4) given by Crank [50] for a purely Fickian diffusion:

$$\begin{aligned} M = M_{\infty,1} \times \left\{ 1 - \frac{8}{\pi^2} \sum_{n=0}^{\infty} \frac{1}{(2n+1)^2} \exp\left(-\frac{D_1 (2n+1)^2 \pi^2 t}{l^2} \right) \right\} \\ + M_{\infty,2} \times \left\{ 1 - \frac{8}{\pi^2} \sum_{n=0}^{\infty} \frac{1}{(2n+1)^2} \exp\left(-\frac{D_2 (2n+1)^2 \pi^2 t}{l^2} \right) \right\} \end{aligned} \tag{10}$$

where $M_{\infty,1}$ and $M_{\infty,2}$ represents the total amount of water absorbed or desorbed by the sample at each respective stage. At the temperature T$\leq$200°C in desorption, the moisture diffusion becomes purely Fickian, $D_2 = 0$ and $M_{\infty,2} = 0$.

D_1, $M_{\infty,1}$,D_2, and $M_{\infty,2}$ were identified simultaneously by a standard inverse method. The residual consists of modeled and measured M differences. The residual 2-norm was minimized using the least-square method in MATLAB [54]. This generated excellent fits for all testing conditions (see Figure 5&7 in Section 5). The identified parameters are given in table 2.

In equation (10), D_1 and $M_{\infty,1}$ are interdependent. This interdependence is also valid for D_2 and $M_{\infty,2}$. During the tests, the weight variation stabilization was not reached in the second stage of diffusion. Therefore, the experimental data obtained did not allow a clear identification of D_2 and $M_{\infty,2}$. However, the adopted methodology allows to give an order of magnitude.

Firstly, the table 2 shows a very small variability of $M_{\infty,1}$ as a function of temperature, during desorption tests. This can be explained by the fact that the samples were initially stored in the same ambient condition before the desorption tests. Hence, when they are exposed to a dry environment, they desorbed roughly the same amount of moisture in the first stage regardless of the temperature. Such conclusion cannot be made on the temperature sensitivity in the case of $M_{\infty,2}$, since stabilization was not reached in the second stage.

Secondly, the moisture diffusion coefficients D_1 and D_2 increased with rising temperature. We fitted this temperature dependence with an Arrhenius law:

$$D_1(T) = D_{0,1} \exp\left(-\frac{E_{a,1}}{RT} \right) \tag{11}$$

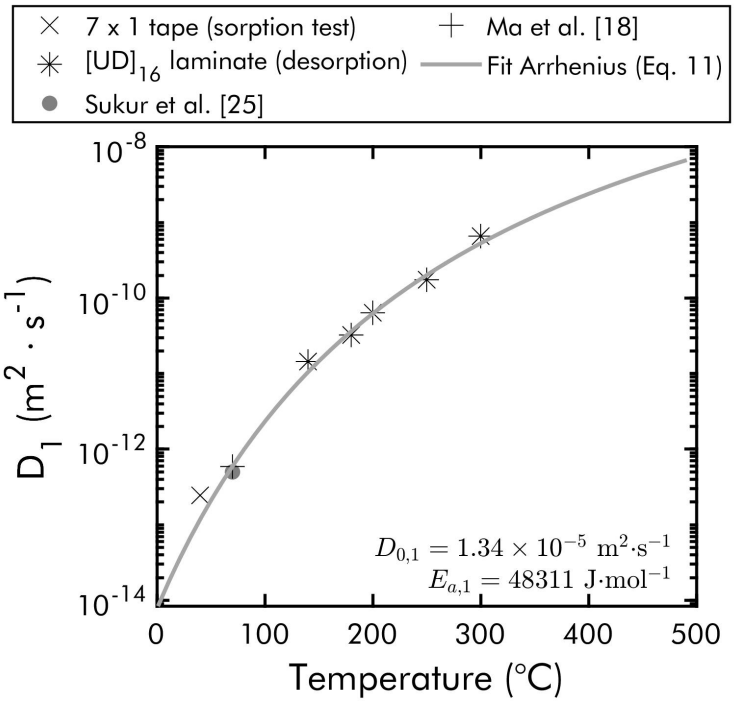

Figure 8: Diffusion coefficients D_1 vs temperature for the first stage of moisture diffusion in CF/PEKK during desorption at high temperatures (star symbols) and sorption at low temperature (cross symbol). Comparison with values obtained from the literature on CF/PEKK [25] and CF/PEEK [18] at 70°C.

where $D_{0,1}$ is a pre exponential constant in $\mathrm{m^2{\cdot}s^{-1}}$, $E_{a,1}$ the activation energy of the first stage of moisture diffusion in $\mathrm{J{\cdot}mol^{-1}}$, R the universal (or perfect) gas constant which is equal to 8.314 $\mathrm{J{\cdot}mol^{-1}{\cdot}K^{-1}}$, and T the temperature in °K.

We determined $D_{0,1}$ and $E_{a,1}$ (Figure 8) with the diffusion coefficients shown in Table 2 and deduced from desorption tests only (140°C - 300°C). In addition, the diffusion coefficient determined experimentally at 40°C during sorption was further used to validate the Arrhenius law estimation at lower temperatures. Results are reported on figure 8.

As shown in Figure 8, a good correlation can be observed between the diffusion coefficients obtained by other authors on CF/PEKK [25] and CF/PEEK [18] and the estimated value with the Arrhenius law (Figure 8). Moreover, there is a small difference between the diffusion coefficient predicted by the Arrhenius trend and the experimental value we determined during the sorption test at 40°C. Such a symmetry sorption-desorption during transient regime is in-line with results already reported in the literature for cured fiber-reinforced epoxy matrix composites [55, 45] and neat PEEK polymer [56, 57]. This implies that the diffusion coefficient can be identified, at a given temperature, by both desorption or sorption tests.

With respect to D_2, its sensitivity to temperature cannot be analyzed from the tests carried out in this study, given the stabilization that has not been reached in the second stage. However, the order of

magnitude obtained from the identification allows to show that D_2 is very low compared to D_1. This means that the moisture diffusion kinetic in the first stage is much faster than the second stage.

7. Discussion

Two different behaviors were observed during the desorption tests. The CF/PEKK samples experiments a Fickian diffusion at T$\leq$ 200°C and a Non-Fickian behavior at T$>$ 200°C. These different behaviors can be explained by how the water molecules were initially stored in the composite samples.

Several studies have been conducted in the literature to understand how water molecules are stored in polymers. There are two main approaches. The first approach is based on the free volume theory proposed by Adamson for epoxy polymers [58]. The second approach takes into account the molecular interactions between the water molecules and the polymer molecules, by assuming that water molecules form hydrogen bonds with hydrophilic sites which are the most polar groups present in the polymer.

Several authors showed that water molecules are stored in the polymer matrix in two forms known as "free" water, diffusing in the free volumes or "bonded" water, temporarily trapped on proton receiver sites present in the molecular network of the polymer [59, 60, 61]. The first approach of free volume is based on the fact that water diffuses into the polymer, occupying essentially the free volumes present in the polymer. Based on this approach, during moisture sorption, the water molecules can diffuse in the free volumes present in the composites or bind with the polymer matrix. The free volumes may be nano or micro porosities located in the polymer matrix or at the fiber - matrix interfaces [45]. These two mechanisms occurring throughout the sorption process lead to the dual stage behavior visible from the desorption curves. The moisture diffusion kinetic during both stages depend on temperature. The desorption of "bonded" water requires sufficient thermal energy. If the thermal energy is insufficient to break the bonds between the water molecules and the polymer, the "bonded" water remains in the material. This may explain the Fickian behavior observed at T$\leq$ 200°C.

However, the first approach does not explain the hydrophobic character of some materials with a large free volume, such as fluoridated and silicone elastomers, or the fact that the water concentration increases when the theoretical free volume fraction decreases for some epoxy-amine polymers [62, 63, 64]. For this reason, another approach based on the interactions between the water molecules and the polar groups within the polymer is also used to explain the dual stage behavior. This approach has been validated in several works where most authors have indeed observed an increase in the water concentration in the polymer with an increase of the concentration of polar groups [65, 66, 67]. In fact, it is assumed that water molecules form two types of hydrogen bonds with the polar groups of the polymer: single bonds and double bonds [68]. The single bonds have an activation energy in desorption around 41840 J·mol^{-1}, and tend to dominate in epoxy polymers. Double bonded water molecules have a higher desorption activation energy (around

62760 J·mol^{-1}) and would be more difficult to desorb from the polymer matrix [23]. The moisture diffusion in the polymer can thus correspond to a "jump" of water molecules from one polar group to another [66]. The kinetics of water diffusion will then depend on the intensity of the hydrogen bonds between the polar groups and the polymer matrix. The stronger these bonds are, the slower the diffusion will be. The major polar group in PEKK resin are the carbonyl (C=O) groups of the ketone function. These groups are considered moderately polar, *i.e.* they are less susceptible to form hydrogen bonds with water. In contrast, hydroxyl groups (predominant in epoxy polymers) can bond easily with water molecules and are thus classified as highly polar.

Based on this second approach, the behaviors observed on the desorption curves can be explained by the polymer-water interactions mentioned above. First, the weight loss observed at the beginning can be attributed to the breaking of single hydrogen bonds between the polymer matrix and dissolved water molecules. As it can be seen on the desorption curves, this first stage is relatively fast. Second, the weight loss stabilization occurs when the thermal energy is insufficient to break the double hydrogen bonds. As soon as the thermal energy becomes high enough, a further weight loss is observed after the first stage, corresponding to the desorption of the doubly bonded water molecules. This second stage is relatively slower compared to the first stage.

Both approaches described in the literature can explain the CF/PEKK behavior under hygrothermal conditions. Since there are generally micro porosities remaining in the composite laminates after consolidation, the free volume approach is not negligible. Perhaps the water diffusion process in CF/PEKK composite is a combination of these two approaches. To prove this, investigations at a micro scale would be necessary. The macro-scale tests performed in this study just highlight the Non-Fickian behavior of CF/PEKK at high temperatures and provide the associated diffusion kinetics.

8. Conclusion

The characterization of moisture diffusion kinetics at high temperatures in high-performance thermoplastic composites has been investigated.

Moisture transport kinetics in TPCs can be characterized by moisture diffusion coefficient. The latter is determined after moisture sorption or desorption test. In the literature, the moisture diffusion coefficient is always determined at low temperature after sorption tests. Since high-performance TPCs are processed at high temperatures, it is necessary to characterize moisture diffusion at temperatures above the glass transition temperature. The existing characterization techniques (TGA, DVS) do not allow to accurately perform desorption tests at high temperatures on representative sample sizes. For this reason, a new device named OMICHA (Online Moisture Ingress CHAracterization) was developed and validated. This new device allowed to measure continuously the weight variation of a sample, of representative size, exposed

to a controlled environment in temperature up to 330°C and humidity. The OMICHA device was used to characterize moisture diffusion kinetics in a high-performance TPC (CF/PEKK) laminate samples initially stored in ambient condition for 5 months.

Thanks to the desorption tests carried out at high temperatures (from 140°C to 300°C), using the OMICHA device, two diffusion mechanisms have been highlighted. Depending on the desorption temperature, the diffusion is either Fickian or Non-Fickian. This dual behavior was described, with a good correlation, by a dual stage model which is based on a superposition of two simultaneous Fickian diffusion. The dual behavior supports that moisture is indeed stored in the polymer matrix in two forms: "weakly bonded water" and "strongly bonded water". A desorption test in the melting range of the material showed that it is difficult to desorb the strongly bonded water without causing material degradation.

Desorption tests also allowed the evaluation of moisture diffusion coefficients in the composite sample at high temperatures. As mentioned in other works in the literature, the diffusion is thermally activated and follows an Arrhenius type law. The characterization of the moisture diffusion kinetics at high temperatures has shown that the diffusion coefficients even at high temperatures are very low and largely lower than the thermal diffusivity (between 10^{-6} and $10^{-7}\mathrm{m}^2{\cdot}\mathrm{s}^{-1}$ [69]). Moisture diffusion is thus slower than heat diffusion in CF/PEKK.

These results call into question the low temperature (below 160°C) of drying protocols often used during the processing of high-performance TPCs. At these low temperatures, only part of the stored water is desorbed. The other part, strongly bonded to the polymer, remains in the material. This residual water can eventually form nucleation sites for porosities during the processing of the material and lead to the formation of defects (voids, delamination, *etc.*) in the final part. The drying protocols used prior to processing must take into account these slow diffusion kinetics and dual stage behavior, to achieve effective drying.

Appendix A. Supplementary materials

Figure A.9 (left) shows the internal part of the sample holder and the salt solution container placed in the oven. Figure A.9 (right) shows the weight variation Δw of the sample holder at 40°C and 65 %RH before the sample positioning. Under constant temperature and hygrothermal conditions, the sample holder does not experiment a significant weight variation.

Acknowledgments

The authors would like to acknowledge the funding of PERFORM project led by IRT Jules Verne (French Institute for Advanced Research and Technology Manufacturing technologies for composites, metals and Hybrid Structures) who made this work possible. Authors wish to associate the industrial partners

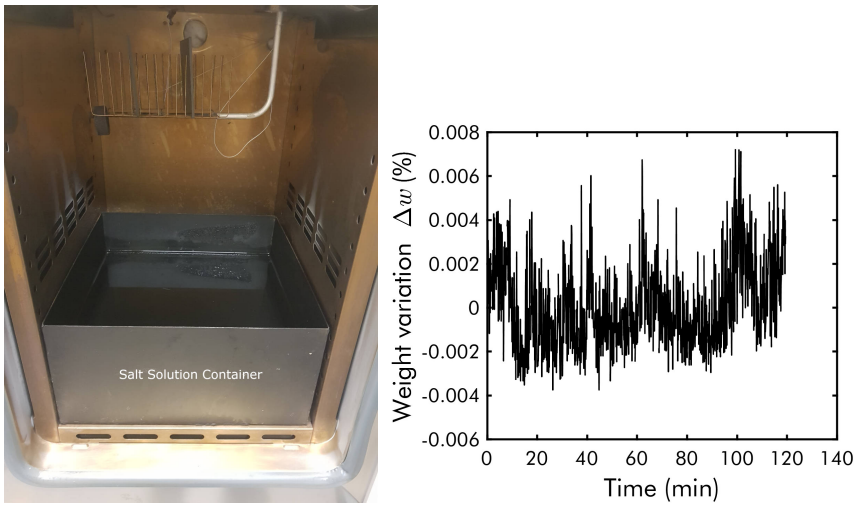

Figure A.9: Internal picture of OMICHA bench showing the internal part of the sample holder and the salt solution container (left). Evolution of the weight variation Δw of the sample holder at 40°C and 65 %RH before sample positioning (right).

of PERFORM project: Airbus, Daher, Safran, Latecoere, Stelia Aerospace, Clayens NP, Naval Group and Faurecia.

The authors would like to thank two colleagues without whom the OMICHA setup would not have been functional. Nicolas Lefevre helped with the setup design and assembly and Julien Aubril helped with the acquisition and control of the bench.

[1] CD Shirrell and J Halpin. Moisture absorption and desorption in epoxy composite laminates. In *Composite Materials: Testing and Design (Fourth Conference)*. ASTM International, 1977.

[2] Alfred C Loos and George S Springer. Moisture absorption of graphite-epoxy composites immersed in liquids and in humid air. *Journal of composite materials*, 13(2):131–147, 1979.

[3] E Pérez-Pacheco, JI Cauich-Cupul, A Valadez-González, and PJ Herrera-Franco. Effect of moisture absorption on the mechanical behavior of carbon fiber/epoxy matrix composites. *Journal of materials science*, 48(5):1873–1882, 2013.

[4] Jack R Vinson. *Advanced composite materials-environmental effects*. ASTM International, 1978.

[5] LK Grunenfelder and SR Nutt. Void formation in composite prepregs–effect of dissolved moisture. *Composites Science and Technology*, 70(16):2304–2309, 2010.

[6] JL Kardos, MP Duduković, and R Dave. Void growth and resin transport during processing of thermosetting—matrix composites. *Epoxy resins and composites IV*, pages 101–123, 1986.

[7] G Fernlund, J Wells, L Fahrang, J Kay, and A Poursartip. Causes and remedies for porosity in composite manufacturing. In *IOP conference series: materials science and engineering*, volume 139, page 012002. IOP Publishing, 2016.

[8] G Dorey, SM Bishop, and PT Curtis. On the impact performance of carbon fibre laminates with epoxy and peek matrices. *Composites Science and Technology*, 23(3):221–237, 1985.

[9] R Selzer and K Friedrich. Mechanical properties and failure behaviour of carbon fibre-reinforced polymer composites under the influence of moisture. *Composites Part A: Applied Science and Manufacturing*, 28(6):595–604, 1997.

[10] Ping Zhou, Jingwei Tian, Chenggao Li, and Zhecheng Tang. Comparative study of durability behaviors of thermoplastic polypropylene and thermosetting epoxy exposed to elevated temperature, water immersion and sustained bending loading. *Polymers*, 14(14):2953, 2022.

[11] R Delasi and JB Whiteside. *Effect of moisture on epoxy resins and composites.* ASTM International, 1978.

[12] A Zafar, Fabio Bertocco, J Schjødt-Thomsen, and JC Rauhe. Investigation of the long term effects of moisture on carbon fibre and epoxy matrix composites. *Composites Science and Technology*, 72(6):656–666, 2012.

[13] Marco Lai, J Botsis, Joel Cugnoni, and D Coric. An experimental–numerical study of moisture absorption in an epoxy. *Composites part A: applied science and manufacturing*, 43(7):1053–1060, 2012.

[14] Corentin Humeau, Peter Davies, and Frédéric Jacquemin. Moisture diffusion under hydrostatic pressure in composites. *Materials & Design*, 96:90–98, 2016.

[15] Basile de Parscau du Plessix, Frédéric Jacquemin, Patrice Lefébure, and Steven Le Corre. Characterization and modeling of the polymerization-dependent moisture absorption behavior of an epoxy-carbon fiber-reinforced composite material. *Journal of Composite Materials*, 50(18):2495–2505, 2016.

[16] Chaogan Gao and Chuwei Zhou. Moisture absorption and cyclic absorption–desorption characters of fibre-reinforced epoxy composites. *Journal of materials science*, 54(11):8289–8301, 2019.

[17] Sang Yoon Park, Won Jong Choi, Chi Hoon Choi, and Heung Soap Choi. An experimental study into aging unidirectional carbon fiber epoxy composite under thermal cycling and moisture absorption. *Composite Structures*, 207:81–92, 2019.

[18] Chen-Chi M Ma and Shih-Wen Yur. Environmental effects on the water absorption and mechanical properties of carbon fiber reinforced pps and peek composites. part ii. *Polymer Engineering & Science*, 31(1):34–39, 1991.

[19] Chen-Chi M Ma, Chang-Lun Lee, Min-Jong Chang, and Nyan-Hwa Tai. Hygrothermal behavior of carbon fiber-reinforced poly (ether ether ketone) and poly (phenylene sulfide) composites. i. *Polymer composites*, 13(6):448–453, 1992.

[20] Li Zhang and MR Piggott. Water absorption and fiber-matrix interface durability in carbon-peek. *Journal of Thermoplastic Composite Materials*, 13(2):162–172, 2000.

[21] Yun Hae Kim, Sung Won Yoon, Jin Woo Lee, Jin Cheol Ha, and Ri Ichi Murakami. Effect of moisture absorption and fiber ply orientation for artificial hip joint on the mechanical properties of carbon/peek composites. In *Advanced Materials Research*, volume 774, pages 1326–1335. Trans Tech Publ, 2013.

[22] Toufik Saoudi and Mohamed El Amine Belouchrani. Mechanical properties and diffusion behavior of carbon fiber-reinforced peek on exposure to heat and water. *Composites: Mechanics, Computations, Applications: An International Journal*, 10 (4), 2019.

[23] Emilie Courvoisier. *Analyse et modélisation cinétique du vieillissement thermique des matrices PEI et PEEK et ses conséquences sur l'absorption d'eau.* PhD thesis, Paris, ENSAM, 2017.

[24] Kyo-Moon Lee, Soo-Jeong Park, Tianyu Yu, Seong-Jae Park, and Yun-Hae Kim. Experimental prediction of internal defects according to defect area on ndi via water absorption behavior. *International Journal of Modern Physics B*, 35 (14n16):2140021, 2021.

[25] Emine Feyza Sukur, Sinem Elmas, Mahsa Seyyednourani, Volkan Eskizeybek, Mehmet Yildiz, and Hatice S Sas. A rational study on the hydrothermal aging of afp manufactured cf/polyetherketoneketone composites with in situ consolidation supported by acoustic emission inspection. *Journal of Applied Polymer Science*, page e52480, 2022.

[26] Rogerio L Mazur, Pedro C Oliveira, Mirabel C Rezende, and Edson C Botelho. Environmental effects on viscoelastic behavior of carbon fiber/pekk thermoplastic composites. *Journal of Reinforced Plastics and Composites*, 33(8):749–757, 2014.

[27] Rogério L Mazur, Geraldo M Cândido, Mirabel C Rezende, and Edson C Botelho. Accelerated aging effects on carbon fiber pekk composites manufactured by hot compression molding. *Journal of Thermoplastic Composite Materials*, 29(10): 1429–1442, 2016.

[28] Jaehyong Jeong, Daesung Lee, Hyunwoo Ju, Jinhwe Kweon, and Youngwoo Nam. Effect of hygrothermal condition on single-lab shear behavior of induction-welded cf/pekk thermoplastic composites. *Advanced Composite Materials*, pages 1–17, 2022.

[29] Xavier Colin and Jacques Verdu. Humid ageing of organic matrix composites. In *Durability of composites in a marine environment*, pages 47–114. Springer, 2014.

[30] Jalal El Yagoubi, Gilles Lubineau, Frederic Roger, and Jacques Verdu. A fully coupled diffusion-reaction scheme for moisture sorption–desorption in an anhydride-cured epoxy resin. *Polymer*, 53(24):5582–5595, 2012.

[31] Luigi Calabrese, Vincenzo Fiore, Elpida Piperopoulos, Dionisio Badagliacco, Davide Palamara, Antonino Valenza, and Edoardo Proverbio. In situ monitoring of moisture uptake of flax fiber reinforced composites under humid/dry conditions. *Journal of Applied Polymer Science*, 139(16):51969, 2022.

[32] Halina Garbalińska, Magdalena Bochenek, Winfried Malorny, and Julia von Werder. Comparative analysis of the dynamic vapor sorption (dvs) technique and the traditional method for sorption isotherms determination — exemplified at autoclaved aerated concrete samples of four density classes. *Cement and Concrete Research*, 91:97–105, 2017. ISSN 0008-8846.

[33] Sneha Sheokand, Sameer R Modi, and Arvind K Bansal. Dynamic vapor sorption as a tool for characterization and quantification of amorphous content in predominantly crystalline materials. *Journal of pharmaceutical sciences*, 103(11): 3364–3376, 2014.

[34] Dynamic Vapour Sorption apparatus. Surface measurement systems. `https://www.surfacemeasurementsystems.com/products/dynamic-vap` Accessed: 2022-10-03.

[35] Helena Perez-Martin, Paul Mackenzie, Alex Baidak, Conchúr M Ó Brádaigh, and Dipa Ray. Crystallinity studies of pekk and carbon fibre/pekk composites: A review. *Composites Part B: Engineering*, 223:109127, 2021.

[36] Julien Avenet. *Assemblage par fusion de composites à matrice thermoplastique: Caractérisation expérimentale et modélisation de la cinétique d'auto-adhésion hors équilibre*. PhD thesis, Université de Nantes (UN), 2021.

[37] Helena Pérez-Martín, Paul Mackenzie, Alex Baidak, Conchúr M Ó Brádaigh, and Dipa Ray. Crystallisation behaviour and morphological studies of pekk and carbon fibre/pekk composites. *Composites Part A: Applied Science and Manufacturing*, page 106992, 2022.

[38] Nigel CW Judd. Absorption of water into carbon fibre composites. *British Polymer Journal*, 9(1):36–40, 1977.

[39] Michelle Leali Costa, Mirabel Cerqueira Rezende, and Sergio Frascino M De Almeida. Effect of void content on the moisture absorption in polymeric composites. *Polymer-Plastics Technology and Engineering*, 45(6):691–698, 2006.

[40] Sang Yoon Park, Won Jong Choi, and Heung Soap Choi. The effects of void contents on the long-term hygrothermal behaviors of glass/epoxy and glare laminates. *Composite Structures*, 92(1):18–24, 2010.

[41] I. Arganda-Carreras, V. Kaynig, C. Rueden, K. W. Eliceiri, J. Schindelin, A. Cardona, and H. Sebastian Seung. Trainable weka segmentation: a machine learning tool for microscopy pixel classification. *Bioinformatics*, 33:2424–2426, 2017.

[42] David Paganin, Sheridan C Mayo, Tim E Gureyev, Peter R Miller, and Steve W Wilkins. Simultaneous phase and amplitude extraction from a single defocused image of a homogeneous object. *Journal of microscopy*, 206(1):33–40, 2002.

[43] Lewis Greenspan. Humidity fixed points of binary saturated aqueous solutions. *Journal of research of the National Bureau of Standards. Section A, Physics and chemistry*, 81(1):89, 1977.

[44] Miroslav Čekon and Ondřej Šikula. Experimental and numerical study on the thermal performance of polycarbonate panels. *Journal of Building Engineering*, 32:101715, 2020.

[45] Y Jack Weitsman. *Fluid effects in polymers and polymeric composites*. Springer Science & Business Media, 2011.

[46] Lisa Feuillerat, Olivier De Almeida, Jean-Charles Fontanier, and Fabrice Schmidt. Effect of poly (ether ether ketone) degradation on commingled fabrics consolidation. *Composites Part A: Applied Science and Manufacturing*, 149:106482, 2021.

[47] Parina Patel, T Richard Hull, Richard W McCabe, Dianne Flath, John Grasmeder, and Mike Percy. Mechanism of thermal decomposition of poly (ether ether ketone)(peek) from a review of decomposition studies. *Polymer degradation and stability*, 95(5):709–718, 2010.

[48] Chris Croshaw, Levi Hamernik, Lina Ghanbari, Andrea Browning, and Jeffrey Wiggins. Melt-state degradation mechanism of poly (ether ketone ketone): the role of branching on crystallization and rheological behavior. *Polymer Degradation and Stability*, 200:109968, 2022.

[49] Dae-Won Suh, Mi-Kyung Ku, Jae-Do Nam, Byung-Sun Kim, and Sung-Chul Yoon. Equilibrium water uptake of epoxy/carbon fiber composites in hygrothermal environmental conditions. *Journal of Composite materials*, 35(3):264–278, 2001.

[50] John Crank. *The mathematics of diffusion*. Oxford university press, 1979.

[51] Harris G Carter and Kenneth G Kibler. Langmuir-type model for anomalous moisture diffusion in composite resins. *Journal of composite materials*, 12(2):118–131, 1978.

[52] Mark D Placette, Xuejun Fan, Jie-Hua Zhao, and Darvin Edwards. Dual stage modeling of moisture absorption and desorption in epoxy mold compounds. *Microelectronics Reliability*, 52(7):1401–1408, 2012.

[53] H Shirangi, J Auersperg, M Koyuncu, H Walter, WH Muller, and B Michel. Characterization of dual-stage moisture diffusion, residual moisture content and hygroscopic swelling of epoxy molding compounds. In *EuroSimE 2008-International Conference on Thermal, Mechanical and Multi-Physics Simulation and Experiments in Microelectronics and Micro-Systems*, pages 1–8. IEEE, 2008.

[54] MATLAB(R2022a). The mathworks inc., 2022.

[55] David A Bond. Moisture diffusion in a fiber-reinforced composite: part i–non-fickian transport and the effect of fiber spatial distribution. *Journal of Composite Materials*, 39(23):2113–2141, 2005.

[56] Michael A Grayson and Clarence J Wolf. The solubility and diffusion of water in poly (aryl-ether-ether-ketone)(peek). *Journal of Polymer Science Part B: Polymer Physics*, 25(1):31–41, 1987.

[57] G Mensitieri, A Apicella, JM Kenny, and L Nicolais. Water sorption kinetics in poly (aryl ether ether ketone). *Journal of applied polymer science*, 37(2):381–392, 1989.

[58] Michael J Adamson. Thermal expansion and swelling of cured epoxy resin used in graphite/epoxy composite materials. *Journal of materials science*, 15(7):1736–1745, 1980.

[59] Sylvain Popineau, Corinne Rondeau-Mouro, Christine Sulpice-Gaillet, and Martin ER Shanahan. Free/bound water absorption in an epoxy adhesive. *Polymer*, 46(24):10733–10740, 2005.

[60] G Mensitieri, M Lavorgna, P Musto, and G Ragosta. Water transport in densely crosslinked networks: A comparison between epoxy systems having different interactive characters. *Polymer*, 47(25):8326–8336, 2006.

[61] Hyoe Hatakeyama and Tatsuko Hatakeyama. Interaction between water and hydrophilic polymers. *Thermochimica acta*, 308(1-2):3–22, 1998.

[62] V Bellenger, J Verdu, and E Morel. Structure-properties relationships for densely cross-linked epoxide-amine systems based on epoxide or amine mixtures. *Journal of materials science*, 24(1):63–68, 1989.

[63] FX Perrin, Minh Hanh Nguyen, and JL Vernet. Water transport in epoxy–aliphatic amine networks–influence of curing cycles. *European Polymer Journal*, 45(5):1524–1534, 2009.

[64] G Bouvet, Nguyen Dang, S Cohendoz, X Feaugas, S Mallarino, and Sébastien Touzain. Impact of polar groups concentration and free volume on water sorption in model epoxy free films and coatings. *Progress in Organic coatings*, 96:32–41, 2016.

[65] E Gaudichet-Maurin, F Thominette, and J Verdu. Water sorption characteristics in moderately hydrophilic polymers, part 1: Effect of polar groups concentration and temperature in water sorption in aromatic polysulfones. *Journal of applied polymer science*, 109(5):3279–3285, 2008.

[66] I Merdas, F Thominette, A Tcharkhtchi, and J Verdu. Factors governing water absorption by composite matrices. *Composites Science and technology*, 62(4):487–492, 2002.

[67] A Tcharkhtchi, PY Bronnec, and J Verdu. Water absorption characteristics of diglycidylether of butane diol–3, 5-diethyl-2,

4-diaminotoluene networks. *Polymer*, 41(15):5777–5785, 2000.

[68] Jiming Zhou and James P Lucas. Hygrothermal effects of epoxy resin. part i: the nature of water in epoxy. *Polymer*, 40 (20):5505–5512, 1999.

[69] Mike Coulson, Eric Dantras, Philippe Olivier, Nathalie Gleizes, and Colette Lacabanne. Thermal conductivity and diffusivity of carbon-reinforced polyetherketoneketone composites. *Journal of Applied Polymer Science*, 136(38):47975, 2019.